International Journal of Computational Methods
Vol. 18, No. 6 (2021) 2042002 (14 pages)

DOI: 10.1142/S0219876220420025

World Scientific
www.worldscientific.com

Generalized Fourier's Law and Darcy–Forchheimer Forced/Mixed Convective Flow Towards a Riga Plate with Second-Order Velocity Slip: A Numerical Study

Yu-Ming Chu[*,†,**,‡‡], M. Ijaz Khan[‡,††,‡‡], Sumaira Qayym[§], Seifedine Kadry[¶] and Waqar A. Khan[‖]

[*]*Department of Mathematics, Huzhou University Huzhou 313000, P. R. China*

[†]*Hunan Provincial Key Laboratory of Mathematical Modeling and Analysis in Engineering Changsha University of Science & Technology, Changsha 410114, P. R. China*

[‡]*Department of Mathematics, Riphah International University Faisalabad Campus, Faisalabad 38000, Pakistan*

[§]*Department of Mathematics, Quaid-I-Azam University 45320 Islamabad 44000, Pakistan*

[¶]*Department of Mathematics and Computer Science Beirut Arab University, Beirut, Lebanon*

[‖]*School of Mathematics and Statistics Beijing Institute of Technology Beijing 100081, P. R. China*
[**]*chuyuming@zjhu.edu.cn*
[††]*mikhan@math.qau.edu.pk*

Received 29 December 2019
Accepted 23 July 2020
Published 2 November 2020

A numerical study is developed to examine the behavior of the forced/free convective flow towards a stretchable Riga plate with generalized Fourier's law. The flow is saturated through Darcy–Forchheimer porous space and generated due to linear and second-order velocity slip phenomena. Here, the main consideration is given to the energy equation which is modeled in the presence of generalized Fourier's law and heat generation absorption. Stagnation point is also discussed. Appropriate similarity variables lead to ordinary differential equations. The dimensionless coupled equations i.e., momentum and energy are numerically solved by the Built-in-Shooting method. The obtained results divulge that the velocity field declines versus rising values of Darcy–Forchheimer number. The temperature field of the working fluid boosts versus higher estimation of Eckert number and heat generation/absorption parameter. The important factors i.e., skin friction

[‡‡]Corresponding authors.

coefficient and temperature gradient of this research work are calculated by graphically subject to mixed convection parameter, modified Hartmann number, Prandtl number and heat generation parameter. It is observed from the graphical results that the impact of skin friction is more between the stretched Riga surface and fluid particles in the presence of rising values of mixed convection parameter.

Keywords: Generalized Fourier's law; Darcy–Forchheimer porous space; second-order velocity slip; stretched Riga plate; heat generation/absorption; nonlinear forced/free convection.

1. Introduction

In the recent couple of decades, the fluid flows over a porous space have gained much attention and consideration amongst the investigators, researchers, mathematicians, engineers and physicians due to their valuable and fruitful applications occurring in biomathematics, geophysical systems and chemical and mechanical engineering's. Some important and fruitful applications comprise grain storage, fermentation process, crude oil production, flow of water in reservoirs, ground water and recovery systems and ground water pollution and so many others. Fluid flow by a porous surface is much protuberant in beds of fossil fuels, building thermal insulation ingredients, petroleum materials, heat exchanger, energy storage units, nuclear waste disposal, solar receivers and so forth others [Nield and Bejan (1999); Karniadakis and Beskok (2002); Abbas *et al.* (2020); Muhammad *et al.* (2020a, 2020b); Haddad (2014); Siddiqui and Azim (2020); Khan *et al.* (2020a, 2020b); Zhang *et al.* (2020)]. Considerable attention in the last couple of decades was given to such types of mathematical engineering problems of porous space that modeled under the concept of classical Darcy's law. This law is only valid for lower fluid velocity and smaller porosity means permeability rate. Also, this law is insufficient when boundary constraints and inertial effects happen at larger flow rate. On the other hand, the surpassing of Re (Reynolds number) from solidarity relates to nonlinear liquid flow. In view of such conditions, it is difficult to ignore the impacts of boundary constraints and inertia. In 1901, Forchheimer [1901] replaced the Darcian velocity by square velocity term to visualize the influences of boundary constraints and inertia. In 1946, Muskat [1946] named as Forchheimer term, which consistently holds for high Re. Jha and Kaurangini [2011] calculated new approximate semianalytical results for steady state fluid flow between parallel porous channels. Pal and Mondal [2012] explored the effects of variable viscosity and magnetohydrodynamics on Darcy–Forchheimer optimized flow subject to porous space. Seddeek [2006] utilized the Darcy–Forchheimer free/forced convective flow by a permeable surface in the presence of viscous dissipation, Brownian and thermophoresis diffusions.

Magnetohydrodynamics (MHD, also known as hydro-magnetics or magnetofluid dynamics) is a branch of fluid mechanics (FM) that portrays the electro-hydro-magnetic progressions emerging in magnetized flow (electrically conducting)

affected by magnetic field (MF). In classical MHD, the liquid flow of extremely magnetized liquids could be conquered by an external applied magnetic field (EAMF). The effectual flow control can be accomplished distinctively by implementing the Lorentz force in parallel direction to the wall. Gailitis and Lielausis [1961] structured a device in 1961 called Riga plate (RP) to generate the resistive force (Lorentz force) in the parallel direction of wall. RP is an electro-magnetic actuator which incorporates span wise allied array of alternating permanent magnets and electrodes, fixed on a surface of plate [Avilov (1998); Grinberg (1961)]. It tends to be used to diminish the pressure drag and surface force (friction force) of submarines by averting the boundary layer separation and decay the rate of turbulence layer. Blasius flow stability in the presence of MF and crossed electric boundary layer of RP is examined by Tsinober and Shtern [1967]. Shah *et al.* [2020] worked on generalized Fourier's law in the forced/free convective flow over a stretched surface of RP.

In this research work, we have extended the research work of Shah *et al.* [2020], with extra effects i.e., Darcy-Forchheimer porous medium instead of porous medium and second-order velocity slip over a surface of RP where the RP is fixed at the stretched surface. The flow is saturated via Darcy–Forchheimer porous medium and caused via linear stretching. Appropriate similarity variables leads to ordinary differential equations. Numerical results are computed through Shooting method (bvp4c) [Liu (2011); Khan *et al.* (2017)]. Tlili *et al.* [2020], Hayat *et al.* [2016], Khan *et al.* [2018], Xun *et al.* [2016], Khan *et al.* [2020], Dholey [2018], Khan and Alzahrani [2020] and Gireesha *et al.* [2017] representing the influence of fluid flow subject to various flow geometries.

2. Flow Equations

Here, magnetized second-order velocity slip flow towards a RP is considered, where the flow is saturated due to Darcy–Forchheimer porous medium and generated by linear stretching phenomenon. Nonlinear forced/free convection is considered. The flow is discussed in semi-analytical domain where $y = 0$ highlights the stretched surface and $y \to \infty$ represents the ambient surface. Furthermore, $u = U_w(x) + U_{\text{slip}}$ denotes the stretching velocity with second-order velocity slip effects in x-direction, where $U_w(x) = ax$ the stretching velocity and $U_{\text{slip}} = \frac{2}{3}(\frac{3-a^*l^2}{a^*} - \frac{3}{2}\frac{1-l^2}{K_n})\,\lambda\frac{\partial u}{\partial y} - \frac{1}{4}(l^4 + \frac{2}{K_n^2}(1-l^2))\lambda^2\frac{\partial^2 u}{\partial y^2} = L_1\frac{\partial u}{\partial y} + L_2\frac{\partial^2 u}{\partial y^2}$ the second-order velocity slip of viscous fluid, where $a^*(0 \le a^* \le 1)$ stands for coefficient of momentum accommodation, K_n the Kundsen number $K_n = \frac{\lambda}{l}, \lambda$ molecular mean free path and $l = \min[\frac{1}{K_n}, 1]$ characteristics length subject to Kundsen number. Heat generation/absorption and dissipations effects are accounted. For incompressible liquid, the mathematical form of generalized Fourier's law is addressed as

$$\mathbf{q} + \delta_E(\mathbf{V}\cdot\nabla\mathbf{q} - \mathbf{q}\cdot\nabla\mathbf{V}) = -\mathbf{k}\nabla\mathbf{T}. \tag{1}$$

Note that $\mathbf{V}, \mathbf{q}, \delta_E, \nabla, T$ and k highlight the perfect velocity of fluid, heat flux, thermal relaxation time, del operator, temperature and thermal conductivity, respectively. In view of the above equation in mind, we have the following governing expressions:

$$\frac{\partial u}{\partial x} + \frac{\partial v}{\partial y} = 0, \tag{2}$$

$$\left.\begin{aligned} u\frac{\partial u}{\partial x} + v\frac{\partial u}{\partial y} = U_e\frac{\partial U_e}{\partial x} + \nu\frac{\partial^2 u}{\partial y^2} + \frac{\pi J_o Q}{8\rho}\exp\left[-\frac{\pi}{a_1}y\right] \\ - \frac{\nu}{K^*}(u - U_e) - F(u^2 - U_e^2) \\ + g(\beta_1(T - T_\infty) + \beta_2(T - T_\infty)^2), \end{aligned}\right\} \tag{3}$$

$$\left.\begin{aligned} u\frac{\partial T}{\partial x} + v\frac{\partial T}{\partial y} + \delta_E\left[\begin{aligned} &u\frac{\partial u}{\partial x}\frac{\partial T}{\partial x} + v\frac{\partial v}{\partial y}\frac{\partial T}{\partial y} + u\frac{\partial v}{\partial x}\frac{\partial T}{\partial y} + v\frac{\partial u}{\partial y}\frac{\partial T}{\partial x} \\ &+ 2uv\frac{\partial^2 T}{\partial y \partial x} + u^2\frac{\partial^2 T}{\partial x^2} + v^2\frac{\partial^2 T}{\partial y^2} - \frac{Q^*}{\rho c_p}\left(u\frac{\partial T}{\partial x} + v\frac{\partial T}{\partial y}\right) \\ &- \frac{\mu}{\rho c_p}\left(2u\frac{\partial u}{\partial y}\frac{\partial^2 u}{\partial x \partial y} + 2v\frac{\partial u}{\partial y}\frac{\partial^2 u}{\partial y^2}\right) \end{aligned}\right] \\ = \frac{k}{\rho c_p}\frac{\partial^2 T}{\partial y^2} + \frac{\mu}{\rho c_p}\left(\frac{\partial u}{\partial y}\right)^2 + \frac{Q^*}{\rho c_p}(T - T_\infty), \end{aligned}\right\} \tag{4}$$

$$\left.\begin{aligned} u = U_w(x) + U_{\text{slip}}, \quad v = 0, \quad T = T_w \quad \text{at } y = 0 \\ u = U_e = bx, \quad T \to T_\infty \quad \text{as } y \to \infty \end{aligned}\right\}. \tag{5}$$

Note that ν indicates the kinematic viscosity, u, v velocity components, π the constant $(\pi = 3.1416), x, y$ the Cartesian coordinates, U_e the free stream velocity, J_0 current density in electrodes, ρ density, $Q(= M_0 x)$ permanent variable magnets magnetization, a_1 width of the magnets between the electrodes, exp exponential function, $F(= \frac{C_b^*}{xK^{*\frac{1}{2}}})$ coefficient of nonuniform inertia, β_1, β_2 the linear/nonlinear thermal expansion coefficients, C_b^* drag coefficient, g gravitational acceleration, T temperature, δ_E thermal relaxation time, T_∞ ambient temperature, c_p specific heat, Q^* heat generation/absorption coefficient, k thermal conductivity, T_w wall temperature, μ dynamic viscosity and a, b positive constant or stretching rates.

Let

$$u = axf'(\eta), \quad v = -\sqrt{a\nu}f(\eta), \quad \theta = \frac{T - T_\infty}{T_w - T_\infty}, \quad \eta = \sqrt{\frac{a}{\nu}}y. \tag{6}$$

After implementing Eq. (6), we have the following dimensionless equations:

$$f''' + f'' - f'^2 + S^2 + M\exp[-B\eta] + \lambda\theta(1+\beta_t\theta) - \beta^*(f'-S) - \mathrm{Fr}(f'^2 - S) = 0, \tag{7}$$

$$\theta'' + \mathrm{Pr}(Ecf''^2 + \gamma(ff'\theta' - f^2\theta'' - \delta f\theta') - 2\gamma\mathrm{Ec}(f'f''^2 - ff''f''') + \delta\theta + f\theta') = 0, \tag{8}$$

$$\left.\begin{aligned} &f(0) = 0, \quad f'(0) = 1 + \gamma_1 f''(0) + \gamma_2 f'''(0), \quad f'(\infty) = S, \\ &\theta(0) = 1, \quad \theta(\infty) = 0. \end{aligned}\right\} \tag{9}$$

Note that $M(=\frac{\pi J_o M_o}{8\rho a^2})$ indicates the modified Hartmann number, $\beta^*(\frac{v}{aK^*})$ the porosity parameter, $S(=\frac{b}{a})$ the ratio parameter, $\mathrm{Fr}(=\frac{C_b^*}{K^{*\frac{1}{2}}})$ the Darcy–Forchheimer number, $\lambda(=\frac{g\beta_1(T_w-T_\infty)}{a^2x})$ the mixed convection parameter, $\beta_t(=\frac{\beta_2(T_w-T_\infty)}{\beta_1})$ the nonlinear thermal convection variable, $B(=\frac{\pi}{a_1}\sqrt{\frac{\nu}{a}})$ the non-dimensional parameter, $\mathrm{Ec}(=\frac{u_w^2}{c_p(T_w-T_\infty)})$ the Eckert number, $\delta(=\frac{Q^*}{a\rho c_p})$ the heat generation variable, $\mathrm{Pr}(=\frac{\mu c_p}{k^*})$ the Prandtl number, $\gamma(=a\delta_E)$ the thermal relaxation variable, $\gamma_1(=L_1\sqrt{\frac{a}{\nu}}), \gamma_2(=L_2\frac{a}{\nu})$ the first- and second-order slip parameters and $\mathrm{Re}_x(=\frac{U_w x}{\nu})$ the Reynolds number.

The engineering curiosity like skin friction coefficient (C_{fx}) and heat transfer rate (Nu_x) are mathematically defined as

$$\left.\begin{aligned} C_{fx} &= \frac{\tau_w}{\rho U_w^2}, \\ \mathrm{Nu}_x &= \frac{xq_w}{k(T_w - T_\infty)}, \end{aligned}\right\}, \tag{10}$$

where τ_w and q_w indicate the shear stress and heat flux.

The final dimensionless form is

$$\left.\begin{aligned} \mathrm{Re}_x^{0.5} C_{fx} &= f''(0) \\ \mathrm{Re}_x^{-0.5}\mathrm{Nu}_x &= -\theta'(0). \end{aligned}\right\}. \tag{11}$$

3. Discussion

Standard nonlinear (ODEs) Eqs. (7) and (8) with relevant restraints Eq. (9) are disintegrated using a Built-in-Shooting method in Mathematica. This segment elaborates that how consequences of important problem variables comprising magnetic parameter, porosity parameter, ratio parameter, mixed convection parameter, nonlinear convection parameter, heat generation/absorption parameter, Prandtl number, thermal relaxation parameter, first and second velocity slip parameters for skin friction coefficient, velocity field, Nusselt number and temperature distribution through Figs. 1–11 are noteworthy. Characteristics of nonlinear thermal convection parameter against velocity field are scrutinized in Fig. 1. As anticipated, escalation

in nonlinear thermal convection parameter results in contracting the velocity of working fluid and also the momentum layer thickness. Impact of mixed convection parameter on the velocity field is highlighted in Fig. 2. Here, velocity field is growing function of mixed convection parameter. Rising mixed convection parameter

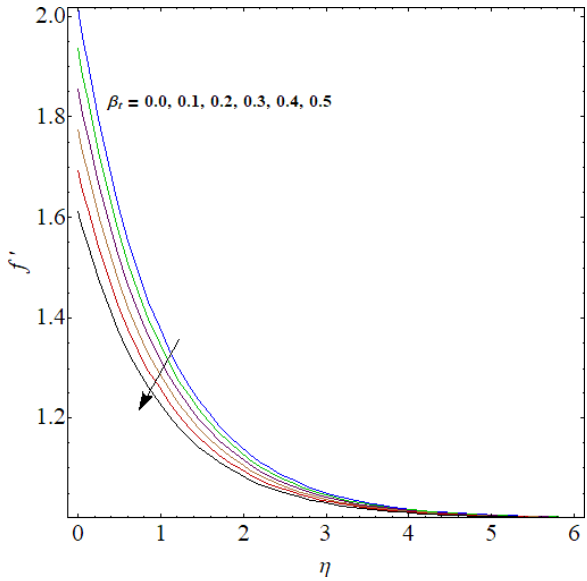

Fig. 1. Behavior of velocity field against nonlinear thermal convection parameter.

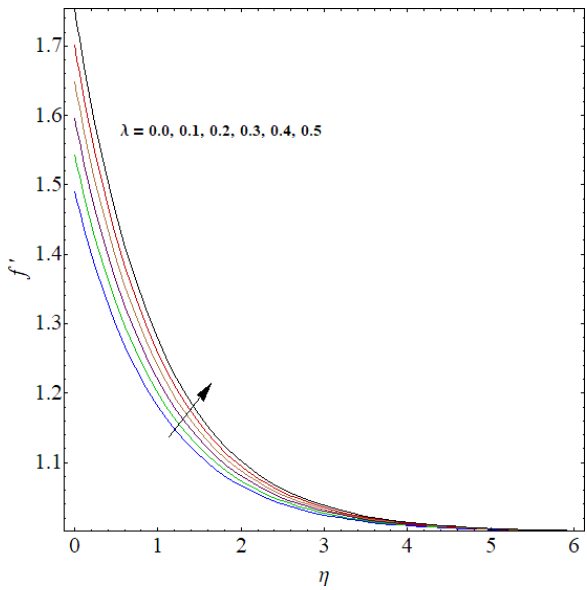

Fig. 2. Behavior of velocity field against mixed convection parameter.

corresponds to larger thermal expansion coefficient which eventually yields velocity field augmentation. Figure 3 unveils second-order slip parameter influence on velocity field. This Figure reported that the rising estimations of second-order velocity slip parameter enhance the velocity of working fluid particles. The deformation

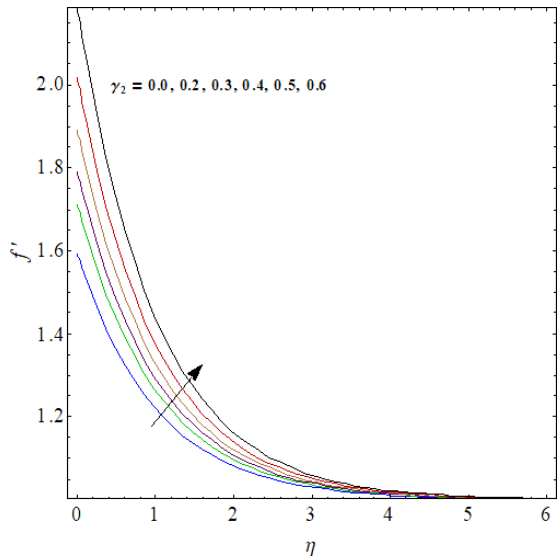

Fig. 3. Behavior of velocity field against second-order velocity slip parameter.

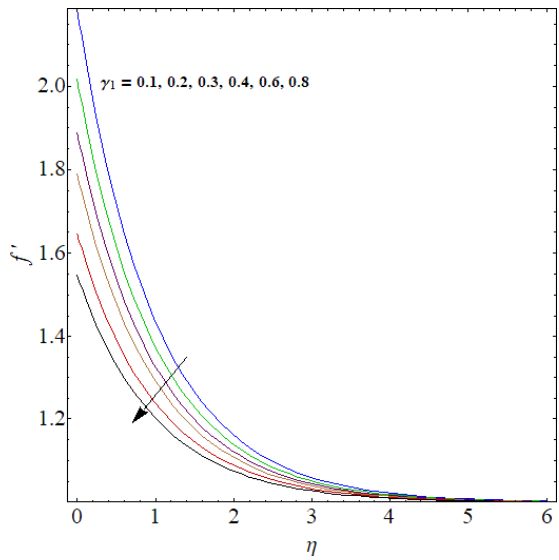

Fig. 4. Behavior of velocity field against first-order velocity slip parameter.

slowly and slowly transferred from the boundary of the stretched surface of sheet to the working fluid and consequently the velocity field increases as the second-order velocity slip parameter takes the maximum range and the remaining all parameters are fixed. The contribution of first-order slip parameter on velocity field is

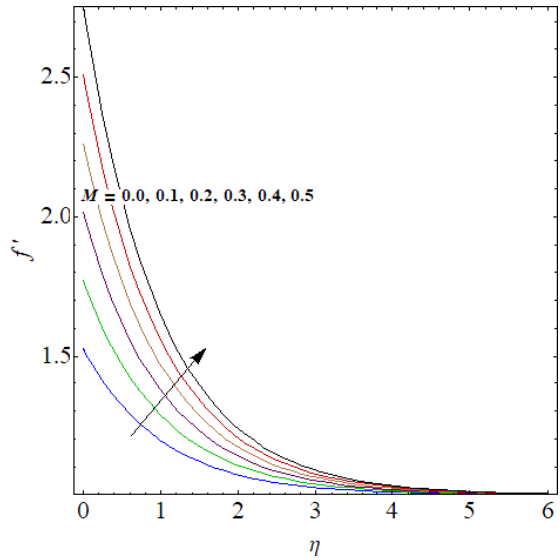

Fig. 5. Behavior of velocity field against magnetic parameter.

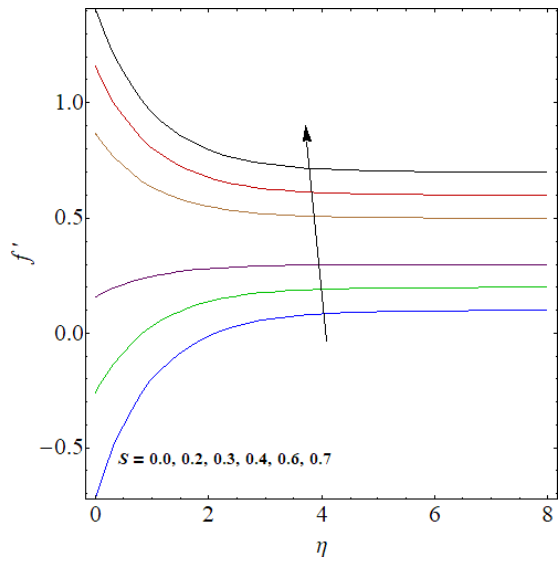

Fig. 6. Behavior of velocity field against velocity ration parameter.

examined through Fig. 4. One can see that velocity field decreases when first-order velocity slip parameter is enlarged. Also, the momentum layer decays versus larger first-order slip parameter. Figure 5 shows the variation of dimensionless velocity field at various rising values of modified magnetic parameter or modified Hartmann

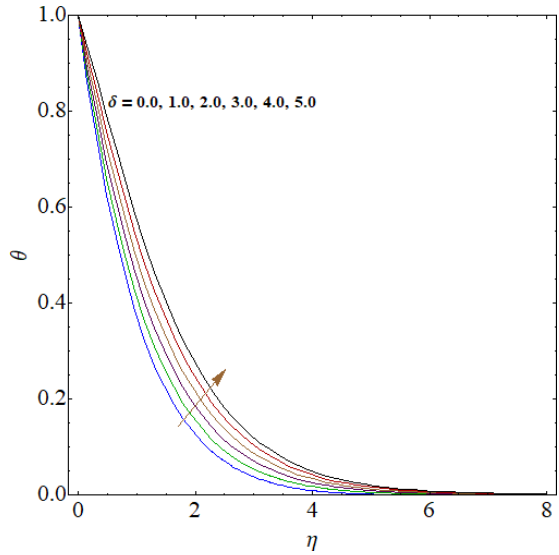

Fig. 7. Behavior of velocity field against heat generation parameter.

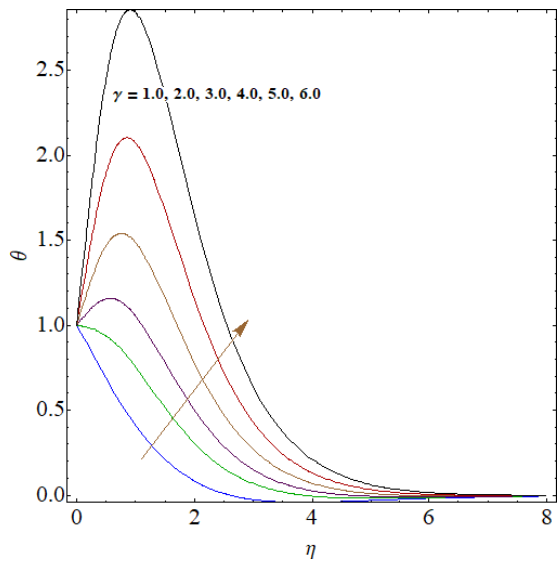

Fig. 8. Behavior of temperature field against thermal relaxation parameter.

number. It is clear that the dimensionless velocity field increase significantly versus higher values of modified Hartmann number. Also, the layer thickness boosts against larger modified Hartmann number. Figure 6 interprets the salient characteristics of ratio parameter on the dimensionless velocity field. It is clearly noticed that

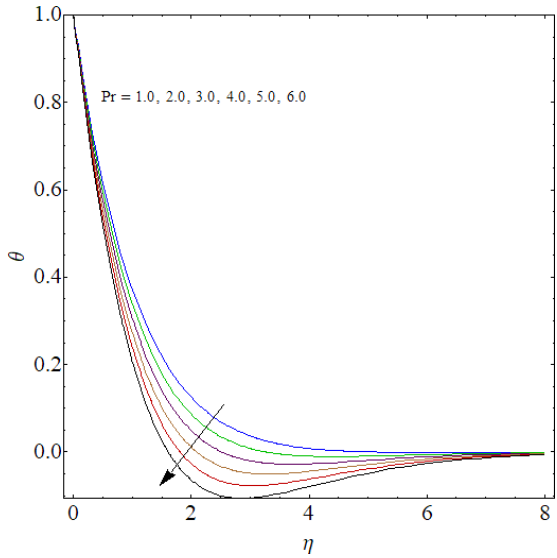

Fig. 9. Behavior of temperature field against Prandtl number.

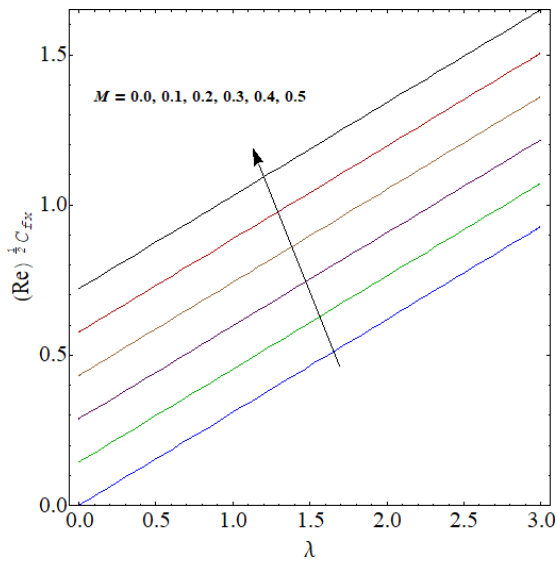

Fig. 10. Behavior of skin friction against magnetic parameter and mixed convection parameter.

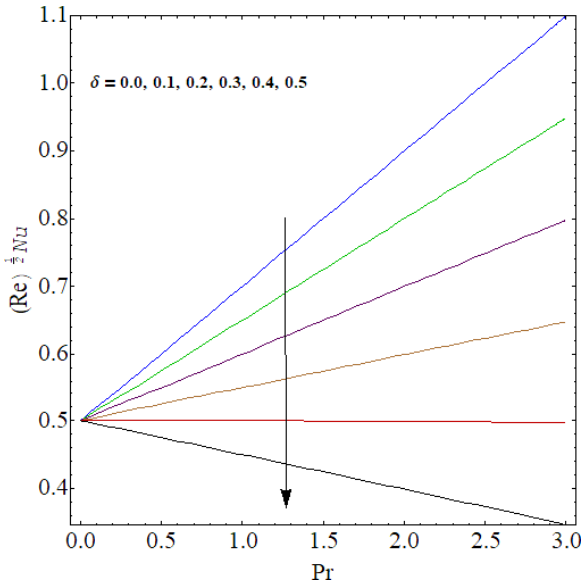

Fig. 11. Behavior of heat transfer rate against heat generation parameter and Prandtl number.

the dimensionless velocity of the viscous working fluid at a stretched RP increases versus higher ratio parameter. The analogous behavior is being observed for heat generation parameter on the thermal distribution in Fig. 7. In physical point of view, the enhancing impact of heat generation parameter upsurge the temperature of the viscous material by a surface of RP, which intensifies the thermal state of the working fluid. Figure 8 depicts the salient attributes of thermal relaxation parameter on the temperature field of viscous field towards a stretched Riga surface. Uplifting the range of thermal relaxation parameter heighten the temperature of viscous working fluid by a stretched surface of RP. It is also remarked that the thermal layer boosts against higher thermal relaxation parameter. The influence of Prandtl number on the dimensionless thermal field and its associated layer thickness is outlined in Fig. 9. Here, both thermal layer and thermal distribution decline against progressive estimations of Prandtl number. The rising impact of Prandtl number diminishes the temperature of working fluid. Mathematically, Prandtl number is the ratio of momentum to thermal diffusivity. The smaller values of Prandtl number, the thermal diffusivity is dominant, while the momentum diffusivity is dominant versus larger Prandtl number. Also, when the Prandtl number upsurges, then the diffusivity associated to thermal field is lesser because the diffusion amount falls. That why the thermal field decays. The physical impact of skin friction coefficient and heat transfer rate i.e., Nusselt number against modified Hartmann number, mixed convection parameter, Prandtl number and heat generation parameter are displayed in Figs. 10 and 11. As anticipated, the skin friction coefficient significantly develops means increases versus larger mixed convection parameter. In Fig. 11,

the heat transfer rate is decreased when we enhance the values of heat generation parameter.

4. Concluding Remarks

A computational work is developed to scrutinize the behavior of forced/free convective flow towards a stretchable RP with generalized Fourier's law. The flow is saturated through Darcy–Forchheimer porous space and generated due to linear and second-order velocity slip phenomena. Here, the main consideration is given to the energy equation which is modeled in the presence of generalize Fourier's law and heat generation absorption. Stagnation point is also discussed. Appropriate similarity variables lead to ordinary differential equations. The dimensionless coupled equations, i.e., momentum and energy are numerically solved by Built-in-Shooting method. The essential facts of the present communication are as follows:

- The velocity field declines versus nonlinear thermal convection parameter.
- The velocity of working fluid over a stretched Riga surface is more versus modified Hartmann number.
- Higher heat generation parameter and thermal relaxation parameter yield larger thermal field.
- A rise in second-order slip parameter corresponds to an enhancement in velocity field.
- Skin friction coefficient is growing function of mixed convection parameter.
- Heat transport is lesser against rising values of heat generation parameter.

Acknowledgment

The research was supported by the National Natural Science Foundation of China (Grant Nos. 11971142, 11871202, 61673169, 11701176, 11626101 and 11601485).

References

Abbas, S. Z., Khan, W.A., Kadry, S. Khan, M. I., Waqas, M. and Khan, M. I. [2020] "Entropy optimized Darcy-Forchheimer nanofluid (silicon dioxide, molybdenum disulfide) subject to temperature dependent viscosity," *Comput. Methods Programs Biomed.* **190**, 105363.

Avilov, V. V. [1998] *Electric and Magnetic Fields for the Riga Plate*, Technical Report, FRZ, Rossendorf.

Dholey, S. [2018] "On the fluid dynamics of unsteady separated stagnation-point flow of a power-law fluid on the surface of a moving flat plate," *Eur. J. Mech.- B/Fluids* **70**, 102–114.

Forchheimer, P. [1901] "Wasserbewegung durch boden," *Zeitschrift des Vereines Deutscher Ingenieure* **45**, 1782–1788.

Gailitis, A. and Lielausis, O. [1961] "On a possibility to reduce the hydrodynamic resistance of a plate in an electrolyte, Applied Magnetohydrodynamics," *Rep. Phys. Institute Riga* **12**, 143.

Gireesha, B. J., Kumar, P. B. S., Mahanthesh, B. Shehzad, S. A. and Rauf, A. [2017] "Nonlinear 3D flow of Casson-Carreau fluids with homogeneous–heterogeneous reactions: A comparative study," *Res. Phys.* **7**, 2762–2770.

Grinberg, E. [1961] "On determination of properties of some potential fields, Applied Magnetohydrodynamics," *Rep. Phys. Institute Riga* **12**, 147–154.

Haddad, S. A. M. [2014] "Thermal instability in Brinkman porous media with Cattaneo-Christov heat flux," *Int. J. Heat Mass Transfer* **68**, 659–668.

Hayat, T., Khan, M. I., Farooq, M., Alsaedi, A., Waqas, M. and Yasmeen, M. [2016] "Impact of Cattaneo-Christov heat flux model in flow of variable thermal conductivity fluid over a variable thicked surface," *Int. J. Heat Mass Transfe* **99**, 702–710.

Khan, I., Ullah, S., Malik, M. Y. and Hussain, A. [2018] "Numerical analysis of MHD Carreau fluid flow over a stretching cylinder with homogenous-heterogeneous reactions," *Res. Phys.* **9**, 1141–1147.

Jha, B. K. and Kaurangini, M. L. [2011] "Approximate analytical solutions for the nonlinear Brinkman-Forchheimer-extended Darcy flow model," *Appl. Math.* **2**, 1432–1436.

Karniadakis, G. and Beskok, A. [2002] *Micro Flows* (Springer, New York).

Khan, M. I. and Alzahrani, F. [2020] "Binary chemical reaction with activation energy in dissipative flow of non-Newtonian nanomaterial," *J. Theor. Comput. Chem.* **19**, 2040006.

Khan, M. I., Alzahrani, F., Hobiny, A. and Ali, Z. [2020a] "Modeling of Cattaneo-Christov double diffusions (CCDD) in Williamson nanomaterial slip flow subject to porous medium," *J. Mater. Res. Technol.* **9**, 6172–6177.

Khan, M. I., Alzahrani, F. and Hobiny, A. [2020b] "Heat transport and nonlinear mixed convective nanomaterial slip flow of Walter-B fluid containing gyrotactic microorganisms," *Alexandria Eng. J.* **59**, 1761–1769.

Khan, M. I., Alzahrani, F. and Hobiny, A. [2020] "Simulation and modeling of second order velocity slip flow of micropolar ferrofluid with Darcy–Forchheimer porous medium," *J. Mater. Res. Technol.* **9** (2020) 7335–7340.

Khan, M. I., Waqas, M., Hayat, T. and Alsaedi, A. [2017] "A comparative study of Casson fluid with homogeneous-heterogeneous reactions," *J. Colloid Interface Sci.* **498**, 85–90.

Liu, C.-S. [2011] "The Lie-group shooting method for boundary-layer problems with suction/injection/reverse flow conditions for power-law fluids," *Int. J. Nonlinear Mech.* **46**, 1001–1008.

Muhammad, R., Khan, M. I., Jameel, M. and Khan, N. B. [2020a] "Fully developed Darcy-Forchheimer mixed convective flow over a curved surface with activation energy and entropy generation," *Comput. Methods Programs Biomed.* **188**, 105298.

Muhammad, R., Khan, M. I., Khan, N. B. and Jameel, M. [2020b] "Magnetohydrodynamics (MHD) radiated nanomaterial viscous material flow by a curved surface with second order slip and entropy generation," *Comput. Methods Programs Biomed.* **189**, 105294.

Muskat, M. [1946] *The Flow of Homogeneous Fluids Through Porous Media* (Edwards, MI).

Nield, D. A. and Bejan, A. [1999] *Convection in Porous Media* (Springer, New York, USA).

Pal, D. and Mondal, H. [2012] "Hydromagnetic convective diffusion of species in Darcy-Forchheimer porous medium with non-uniform heat source/sink and variable viscosity," *Int. Commun. Heat Mass Transfer* **39**, 913–917.

Seddeek, M. A. [2006] "Influence of viscous dissipation and thermophoresis on Darcy-Forchheimer mixed convection in a fluid saturated porous media," *J. Colloid Interface Sci.* **293**, 137–142.

Shah, F., Khan, M. I., Hayat, T., Momani, S. and Khan, M. I. [2020] "Cattaneo-Christov heat flux (CC model) in mixed convective stagnation point flow towards a Riga plate," *Comput. Methods Programs Biomed.* **196**, 105564.

Siddiqui A. M. and Azim, Q. A. [2020] "Creeping flow of a viscous fluid in a uniformly porous slit with porous medium: An application to the diseased renal tubules," *Chin. J. Phys.* **64**, 264–277.

Tlili, I., Bilal, M., Qureshi, M. Z. A. and Abdelmalek, Z. [2020] "Thermal analysis of magnetized pseudoplastic nano fluid flow over 3D radiating non-linear surface with passive mass flux control and chemically responsive species," *J. Mater. Res. Technol.* **9**, 8125–8135.

Tsinober, A. B. and Shtern, A. G. [1967] "Possibility of increasing the flow stability in a boundary layer by means of crossed electric and magnetic fields," *Magnetohydrodynamics* **3**, 103–105.

Xun, S., Zhao, J. , Zheng, L., Chen, X. and Zhang, X. [2020] "Flow and heat transfer of Ostwald-de Waele fluid over a variable thickness rotating disk with index decreasing," *Int. J. Heat Mass Transfer* **103**, 1214–1224.

Zhang, L., Zhuang, W., Khan, N. and Zheng, L. [2020] "Effect of stress relaxation and creep recovery on transportation in porous medium and fracture of the millimeter-scale polymer gel particles for conformance control of heterogeneous oil reservoir," *J. Petroleum Sci. Eng.* **185**, 106648.